

Nanometer-Scale Four-Point Probe Resistance Measurements of Individual Nanowires by Four-Tip STM

S. Hasegawa, T. Hirahara, Y. Kitaoka, S. Yoshimoto, T. Tono and T. Ohba

Abstract We present a review of our recent results about transport properties of nanowires measured by a four-tip scanning tunneling microscope (STM) installed with metal-coated carbon nanotube (CNT) tips. We first present our custom-made apparatus (with UNISOKU Co.) as well as CNT tips, and then some case studies with two different samples, Co-silicide nanowires self-assembled on Si(110) surface and Cu nanowires made by damascene processes used in LSI industry. It is shown that the four-tip STM with CNT tips is versatile and powerful for measuring the conductivity of individual nanostructures.

1 Introduction

Conductivity measurements in sub-micron or nanometer scale are of great interest in nanoscience and nanotechnology. For example, nanoelectronics such as semiconductor devices requires low and stable electrical resistance of interconnects to maintain device performance. Several kinds of methods to measure the conductivity at nanoscales have been developed including fixed electrodes made by microlithography techniques. A method which adopts tips of scanning tunneling

S. Hasegawa (✉) · T. Hirahara · Y. Kitaoka · S. Yoshimoto · T. Tono
Department of Physics, School of Science, University of Tokyo, 7-3-1,
Hongo, Bunkyo-ku, Tokyo 113-0033, Japan
e-mail: shuji@surface.phys.s.u-tokyo.ac.jp

T. Ohba
School of Engineering, University of Tokyo, Tokyo 113-0033, Japan

S. Yoshimoto
Institute of Solid State Physics, University of Tokyo, Kashiwa 277-8581, Japan

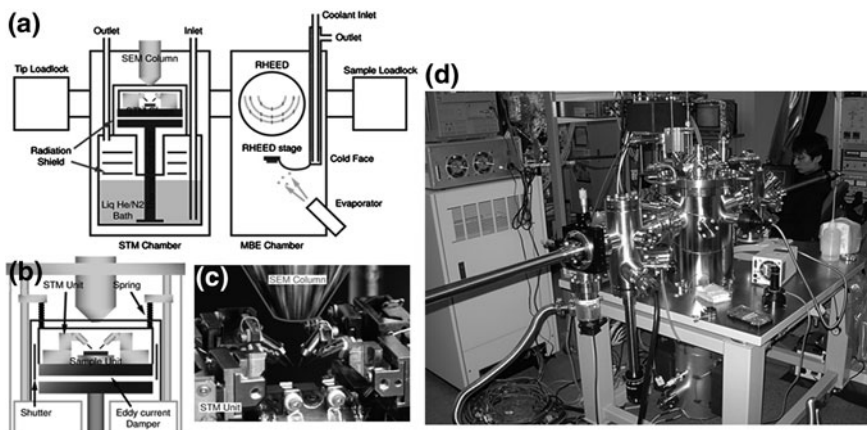


Fig. 1 Schematic drawings of the whole system of low-temperature four-tip STM (a) and around the STM stage (b) [14]. c A close-up photo of the STM stage without radiation shields. d The photo of the whole system

22 microscope (STM) as electrodes, however, has great advantages in positioning of
23 the probes in arbitrary configurations as well as in high spatial resolution of
24 measurements. But single-tip STM is not enough for versatile measurements
25 of transport properties at various kinds of nanostructures: we need source, drain,
26 and gate electrodes. For this reason, several groups [1–10] including companies
27 [11] and our group [12–14] have developed four-tip STM. In which four inde-
28 pendent STM tips are operated in an organic manner with aid of a SEM or optical
29 one, and they are used as electrodes for microscopic two- or four-point probe
30 (μ 4PP) conductance measurements. In this article, we show our apparatuses
31 including installation of carbon nanotube tips [15–17] and some results of resis-
32 tance measurements of nanowires obtained in our group.

33 2 Four-Tip STM System

34 Figures 1a, b show schematic drawings of our new version of four-tip STM system
35 [14], consisting of a main (STM) chamber, a sample preparation molecular beam
36 epitaxy (MBE) chamber, and two load-lock chambers for sample and tip
37 exchanges, all of which are UHV compatible. The STM tips can be installed into
38 the main chamber from the tip load-lock chamber where a hot W filament is
39 installed for out-gassing of the tips. The sample is introduced from the MBE
40 chamber where cleaning of the sample, deposition of materials and reflection-high-
41 energy electron diffraction (RHEED) observation can be done. The sample can be
42 heated by direct current heating and cooled down to about 30 K by continuous-
43 flow type cryostat in the MBE chamber. These capabilities are necessary for

44 preparing aimed surface superstructures, epitaxial thin films, nanodots, nanowires,
45 and for making in situ measurements.

46 The STM stage is mounted on the thermal conducting Cu rod which is soaked
47 in the coolant of the bath cryostat below. The STM stage including the sample and
48 four sets of actuator units is wholly surrounded with two-fold radiation shields and
49 movable shutters. The photo of Fig. 1c is the stage without the radiation shields,
50 and Fig. 1d shows the whole system. The sample and tips can be cooled down to
51 7 K and can be kept for 23 h with liquid He as coolant. In the case of liquid N₂, the
52 minimum temperature is 80 K and the preserved time is longer than three days.

53 The SEM column (APCO Mini-EOC) is mounted above the STM stage. The
54 working distance of SEM is about 25 mm. The electron beam is irradiated from
55 SEM column through a 1 mm diameter hole in the radiation shields. A multi-
56 channel plate for the secondary electron detection for SEM imaging is placed on
57 the inside wall the outer shield. The SEM image is obtained from the secondary
58 electron signal or beam induced current signal electron-beam-induced current
59 image (EBIC). The resolution of the SEM is about 20 nm for both signals.

60 A spring vibration isolator and an eddy-current damper are built between the
61 thermal conductor and the STM stage to avoid vibration of STM stage. The spring
62 isolator decoupled the STM stage from other components. However, during SEM
63 observation, tip/sample exchanges, and cooling the stage, the STM stage is fixed to
64 the thermal conductor (Cu rod) and therefore the isolator and damper are disabled.
65 When we fix the STM stage, the Cu plate works as a thermal conductor and
66 enlarges the contact area for good thermal connection. When we float the STM
67 stage by the springs, this plate makes eddy-current damper. Since alternative
68 arrangements of the small magnets make closed magnetic paths, the magnetization
69 does not affect the SEM beam.

70 Four sets of tip actuator units are mounted at the corner of the square STM
71 stage, and a sample actuator unit is placed at the center. The actuator units consist
72 of stacked piezo ceramics supported by sapphire plates. For fine positioning or
73 scanning in nanometer or sub-nanometer range, tips and samples are driven by
74 conventional piezoelectric effect of the ceramics by DC voltage. The maximum
75 positioning range by this method is about 2 μm to each direction. For coarse
76 positioning, the actuators are driven by stick-slip mechanism in 5 mm travel
77 distance in XY directions and 2.5 mm in Z direction at accuracy of about 100 nm.
78 In addition to these three- or two-dimensional-motion actuators, the tip actuators
79 also contain small piezo ceramics near the tips for fast STM feedback.

80 Figure 2 shows a series of SEM images of the four tips arranged in various
81 configurations [12, 13, 18]. The tips are chemically etched W wires. The probe
82 spacing can be changed from 1 mm to ca. 200 nm in Figs. 2a–c. They can be
83 arranged on a line equidistantly (linear μ4PP method) (c, d) in arbitrary directions,
84 or in square arrangement (square-μ4PP method) Figs. 2e–h. The square can be
85 rotated with respect to the sample surface (rotational square-μ4PP method) by re-
86 positioning each tip under computer control. This is useful to measure anisotropic
87 surface conductivity in which the conductivity is different depending on the crystal
88 orientation.

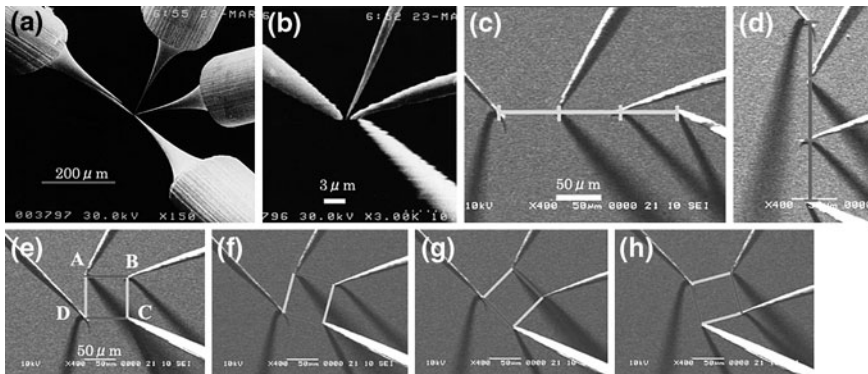


Fig. 2 SEM images of the four W tips in various arrangements in the four-tip STM [12, 13, 18]

3 Metal-Coated Carbon Nanotube Tips

89 An important issue for the four-tip STM is the probe spacing; the probe spacing
90 should be in the order of 10 nm to measure various kinds of nanostructures. At the
91 present the minimum probe spacing in the multi-tip STM is approximately 100 nm
92 when W tips are used. This is due to the radius of tip apex of electrochemically
93 etched W tips. This probe spacing is not small enough for observing ballistic
94 transport and quantum interference effects because the coherence length of con-
95 duction carriers is shorter than 100 nm in many cases. For this reason, continuous
96 efforts are made to shorten the probe spacing down to ca. 10 nm. To make the
97 probe spacing shorter, carbon nanotube tips have been developed in which a
98 carbon nanotube is glued at the end of W tip [19–22]. Since the radius of the
99 (multi-walled) carbon nanotubes is usually ca. 10 nm and the aspect ratio is much
100 higher than usual W tips, two carbon nanotube tips can be brought together into
101 approximately 10 nm spacing. Another feature of the carbon nanotube tip is its
102 mechanical flexibility which can reduce damage to delicate samples such as
103 organic and biological molecules, and make the tips withstand numerous direct
104 contacts to the samples. These properties are quite convenient for the transport
105 measurements by multi-tip STM at nanometer scales. However, there have been
106 problems in the carbon nanotube tips; high contact resistance between the sup-
107 porting metal tip and the attached carbon nanotube strongly disturbs electron
108 transport at the STM/STS measurements. Moreover, adsorbates contained in the
109 carbon nanotube degrade the surface cleanness of the specimen under STM
110 operation.

112 A novel technique for overcoming these difficulties has been developed; the
113 carbon nanotube together with the supporting metal tip is wholly coated with a thin
114 metal layer [15]. Figures 3a,b show TEM images of a W-coated carbon nanotube
115 tip glued on a W supporting tip. The W layer of ca. 3 nm thick was deposited by
116 pulsed laser deposition (PLD) method. The W layer fully covers the tip even at the

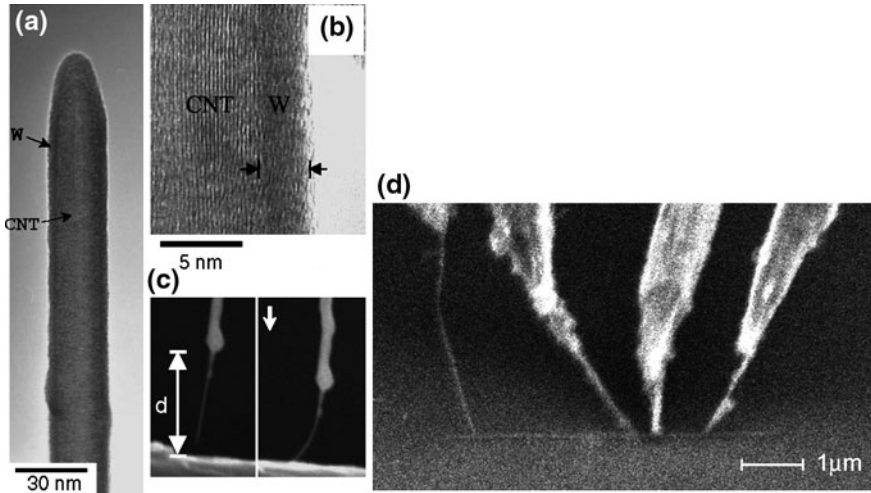


Fig. 3 **a** TEM image and **b** high-resolution TEM image of a W-coated carbon nanotube tip coated by pulsed laser deposition method. **c** SEM images of the W-coated carbon nanotube tip, directly contacting to a sample surface. Reproduced from Ref. [15]. **d** A SEM image showing four carbon nanotube tips contacting a Co-silicide nanowire grown on a Si substrate [23]

117 end. Figure 3c shows flexibility and robustness of the W-coated carbon nanotube
118 tip upon the direct contact to a sample surface. Figure 3d is a SEM image showing
119 four CNT tips contacting a Co-silicide nanowire grown on a Si substrate [23]. We
120 have also confirmed that the electrical resistance at the glued point between the
121 carbon nanotube and supporting W tip is stably reduced by the metal coating;
122 especially PtIr coating is the most efficient for this purpose [16]. Atomic-resolution
123 STM imaging and STS spectra were acquired with the W-coated carbon nanotube
124 tip at the first attempt [15]. With this metal-coated carbon nanotube tips, we have
125 succeeded in bringing the two tips together into less than 30 nm [17, 23, 24]. Since
126 the resolution of SEM is not enough for observing a smaller probe spacing, we
127 believe that the minimum spacing can be reduced to ca. 20 nm, similar to the
128 diameter of CNT itself.

129 4 Measuring Co-Silicide Nanowires

130 CoSi₂ nanowires are known to grow self-assembly by depositing high-purity
131 cobalt on a Si(110) clean surface held at 750–850°C in UHV, as shown in
132 Figs. 4a–c [25]. The nanowires become longer and thinner with lowering the
133 substrate temperature during the Co deposition. The wires are single-crystalline,
134 half of which is embedded in the Si substrate as observed by a cross-sectional
135 TEM image of Fig. 4d [25]. The CoSi₂ is known to be highly conductive metallic

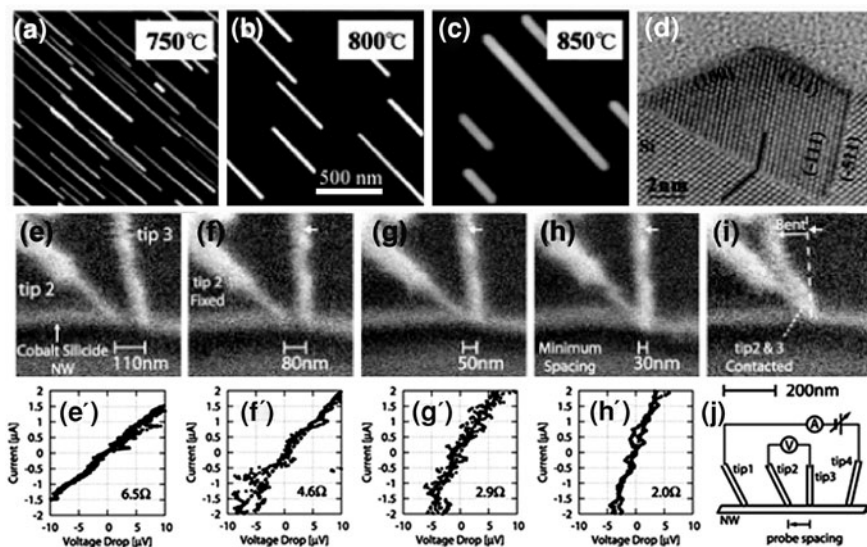


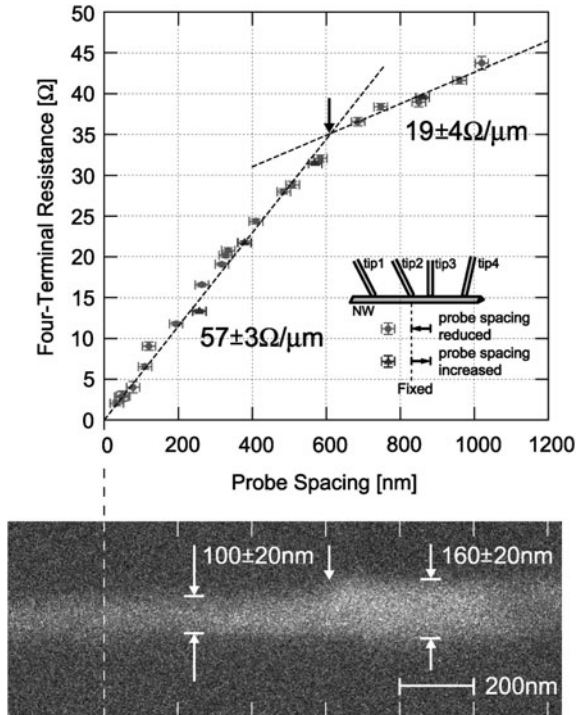
Fig. 4 a–c Atomic force microscopy images of CoSi_2 nanowires formed by depositing Co on the heated Si(110) substrate at different temperatures reproduced [25]. **d** A cross-sectional TEM image of the nanowire from Ref. [25]. **e–h** SEM images of the inner pair of CNT tips (tip 2 and tip 3 in **j**), with different probe spacings, contacting one of the nanowires during the resistance measurements in the four-tip STM [23]. The current probes (tip 1 and tip 4) are about $1 \mu\text{m}$ away from these voltage probes. **e'–h'** Four-terminal current–voltage curves measured at the tip configuration shown in **e–h**, respectively [23]. The four-terminal resistance R_{4t} decreased with reducing the probe spacing. **i** The voltage probes contacted each other, and the tip 3 was bent. **j** A schematic showing the four-terminal current–voltage measurements

136 and its resistivity is $31 \pm 9 \mu\Omega \text{ cm}$ for the nanowire [26] and $\sim 15 \mu\Omega \text{ cm}$ for the
 137 films [27] at 300 K.

138 As shown in Fig. 3d, the four CNT tips were made contact onto one of the
 139 nanowires under SEM observation. The tips were made approach beyond the point
 140 of tunneling until the contact resistances became less than $1 \text{ M}\Omega$, corresponding to
 141 direct contact. At the current–voltage (I – V) measurement, the STM feedback loops
 142 were cut. Even if the tip physically contacted the NW, the contact resistance
 143 between the tip and sample was higher than $50 \text{ k}\Omega$. It was difficult to reduce this
 144 resistance because of the nanometer-sized contact area. This is much larger than
 145 the resistance of the nanowire itself, which is less than $1 \text{ k}\Omega$ with probe spacing
 146 smaller than $1 \mu\text{m}$ [26]. Therefore, by two-terminal I – V measurements, the
 147 resistance did not depend on the probe spacing due to the large contact resistance
 148 at the probe contacts: four-point measurements are indispensable at nanometer
 149 scale.

150 Four-terminal I – V measurements were done by sweeping the bias voltage
 151 between tip 1 and tip 4 with recording the current I and the voltage drop V between
 152 tip 2 and tip 3, with changing the spacing between tip 2 and tip 3 as shown in Figs. 4e–h.
 153 The SEM beam was stopped at the I – V measurements to avoid possible influence on

Fig. 5 The measured four-terminal resistance R_{4t} as a function of the spacing between the voltage probes, and SEM image of the nanowire under measurement (top view). The *black arrow* around 600 nm in the graph and the *white arrow* in the SEM image indicate the position where the nanowire width changes, resulting in a change of the resistivity [23]



154 the resistance caused by high-energy electron beam (10 kV). Figures 4e–h show a
 155 series of SEM images around the voltage probes (tip 2 and tip 3) touching on the
 156 nanowire, and corresponding four-terminal I–V curves are shown in (e'–h').
 157 We reduced the probe spacing between the voltage probes during taking the I–V
 158 characteristics. The positions of the two current probes (tip 1 and tip 4) and one of the
 159 voltage probes (tip 2) were fixed in the measurements, and only tip 3 was shifted. All
 160 I–V curves were linear. The four-terminal resistance $R_{4t} = dV/dI$ around $I = 0$
 161 decreased with shortening the probe spacing. They are several Ω , much smaller than
 162 the contact resistance. A voltage amplifier was introduced at the STM pre-amplifiers
 163 to detect small voltage drops resulted from the small resistance. Finally tip 3 bent as
 164 shown in Fig. 4i, and R_{4t} became 0Ω because of direct contact between the voltage
 165 probes. The minimum probe spacing achieved here was $30 \pm 20 \text{ nm}$ as shown in
 166 Fig. 4h. This was limited by the diameter of the CNT tip apex we used, 30 nm (20 nm
 167 diameter of CNT + 5 nm thick PtIr layer). The error bar in the probe spacing is
 168 determined by the radii of the apices in tip 2 and tip 3.

169 We plot the measured four-terminal resistance R_{4t} as a function of the spacing
 170 between the contact points of the voltage probes on the nanowire in Fig. 5. The
 171 linear proportional relation in the range 30–600 nm means diffusive transport, and
 172 the fit line gives one-dimensional resistivity $\rho_{1D} = 57 \pm 3 \Omega/\mu\text{m}$. By extrapolating
 173 the data points, there seems to be no residual resistance at zero probe

Table 1 Probe spacing L dependence of the four-terminal resistance R_{4t} in various conduction mechanisms

Conduction mechanism	1D Ohmic	2D Ohmic	3D Ohmic	1D strong localization	1D weak localization	Ballistic
L -dependence of R_{4t}	$\propto L^1$	$\propto L^0$ (constant)	$\propto L^{-1}$	$\propto \exp\left(\frac{L}{L_0}\right)$	$\propto \frac{L}{L_0-L}$	$\propto L^0$ (with fluctuation)

L_0 is the localization length

spacing, which is owing to the four-point probe configuration. The gradient decreased to $19 \pm 4 \Omega/\mu\text{m}$ above 600 nm probe spacing. This is due to an increase of the nanowire width from 100 ± 20 to 160 ± 20 nm as shown in the SEM image in Fig. 5. By checking the reproducibility we found that the physical contacts of the CNT tips did not cause any significant damage to the nanowire.

We now discuss the transport property of the NW. Table 1 shows a list of the probe spacing L dependence of the four-terminal resistance in various conduction mechanism. The probe spacing dependence of resistance in CoSi_2 nanowire showed a linear one-dimensional Ohmic feature ($R_{4t} \propto L$). This behavior is due to a one-dimensional conduction path through the nanowire without leakage of current to the underlying three-dimensional substrate or to the two-dimensional substrate surface. This is because a Schottky barrier between the nanowire and the Si substrate confines the current [26]. The mean free path of the electrons in CoSi_2 is around 6 nm at room temperature [28], which is much smaller than the width and height of our nanowire as well as the probe spacing. Therefore, our result of diffusive conduction is reasonable. The three-dimensional resistivity of the nanowire can be calculated. The width of the nanowire is determined by SEM image, and the height can be determined by the transmission electron microscope image [25]. We obtain the three-dimensional resistivity $22 \pm 4 \mu\Omega \text{ cm}$. In the same way, we obtain $19 \pm 4 \mu\Omega \text{ cm}$ for the region larger than 600 nm. These values are comparable to the previous results ($31 \pm 9 \mu\Omega \text{ cm}$) in which similar CoSi_2 NWs were measured with W tips in larger probe spacing range [26].

In the ballistic transport regime, two-terminal and four-terminal resistances (R_{2t} and R_{4t}) do not depend on the probe spacing. They depend only on the total transmission probability T_{23} of electron wavefunction between the voltage probes, tip 2 and tip 3 (which are also the current probes in the two-terminal measurement). A remarkable feature of the ballistic transport is that R_{4t} takes any value between $-R_{2t}$ and $+R_{2t}$, meaning that R_{4t} can be negative by quantum interference effects [21]. At liquid-He temperature, the mean free path of conduction electrons in a CoSi_2 film with the thickness of 110 nm becomes ca. 100 nm [27]. Therefore, at low temperatures, we can possibly observe quantum interference effects in resistance at probe spacing we achieved here by using the PtIr-coated CNT tips. The probe spacing dependence of R_{4t} in the present experiment also excludes observable effects of carrier localization.

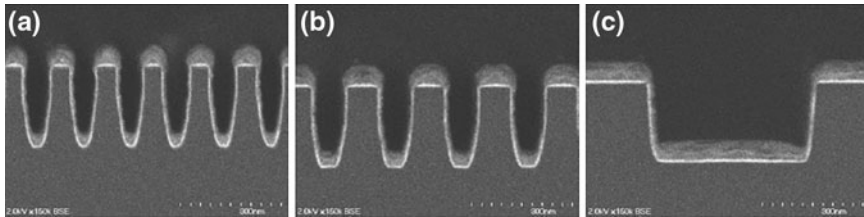


Fig. 6 Cross-sectional SEM image of damascene trenches. The trench widths are **a** 70 nm **b** 100 nm, and **c** 500 nm, respectively [29]

209 5 Measuring Cu Nanowires

210 Copper (Cu) wires are now widely used for interconnects in semiconductor
211 devices. But, as the wire width reaches down to the sub-micrometer scale, which is
212 comparable to the mean free path of conduction electrons in the wires, a significant
213 increase in the resistivity has been observed. This is speculated as due to the
214 increased surface and grain boundary scatterings. As the wire width scales down,
215 electrons will undergo reflections more frequently at the surfaces/interfaces, so the
216 collisions with the surfaces/interfaces will become a significant fraction of the total
217 number of collisions. In addition, grain boundaries in polycrystalline wires may act
218 like partially reflecting planes for electron waves, so they also contribute to the
219 increase of resistivity. To investigate these effects directly, the conductivity
220 measurements by the four-tip STM at nanometer scales is very useful [29].

221 Cu wires having the width between 70 nm and 1 μm were prepared using a Cu/Low-k
222 damascene processes which are now very common in semiconductor industry. Figure 6
223 shows the cross-sectional SEM images of the damascene structure made in SiO_2 layer.
224 Tantalum (Ta) was used as a barrier metal (BM) in this experiment. Cu damascene lines
225 were formed using conventional Cu process such as seed Cu, electrochemical plating
226 (ECP) Cu for trench filling, and chemical-mechanical polishing. The Cu nanowires are
227 not single-crystalline; they are consisted of small gains. By the electron back-scatter
228 diffraction (EBSD) method, such grains are visualized along the Cu damascene lines
229 [29]. The average grain size was measured to be about 100 nm at 70 nm wide Cu
230 nanowires, which did not change so much with the width, because the grain size is
231 thought to be determined by the height when the width is smaller than the height.

232 The four-tip STM was used to measure the resistance of individual wires as
233 shown in Fig. 7. By using Pt-coated CNT tips, the probe spacing can be reduced
234 down to the order of several ten nm routinely [23]. When the Pt-coated CNT tips
235 were used, the contact resistance between the tip and sample could not be smaller
236 than 50 k Ω because of its very small contact area. This means that it is impossible
237 to measure conductive materials whose resistance is less than 50 k Ω by the two-
238 point probe method. Only with the four-point probe method, resistances much
239 smaller than the contact resistance (as small as 0.1 Ω in the present case) can be
240 measured. Therefore, the combination of the CNT tips and the four-tip STM is
241 very powerful for studies in nanoscale measurements.

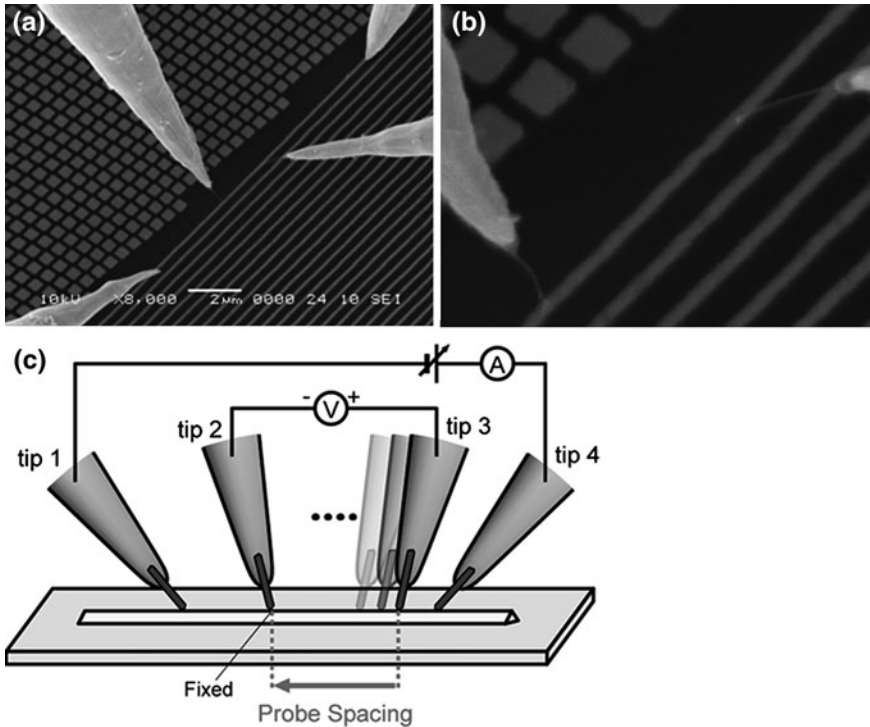


Fig. 7 **a** An SEM image of the Cu wire being contacted with the four probes [29]. **b** The enlargement of the area of rectangle in (a). **c** The illustration of the four-terminal I–V measurement

242 Four-terminal I–V measurements were performed by sweeping the bias voltage
 243 between the outer pair of tips and recording the current I and the voltage drop V
 244 between the inner pair of tips (Fig. 7c). The probe spacing between the voltage
 245 probes was reduced while measuring the I–V characteristics. The two current
 246 probes (tip 1 and tip 4) and one of the voltage probes (tip 2) were fixed during the
 247 measurements, and only tip 3 was moved between tip 2 and tip 4 (Fig. 7c).

248 The measured values of four-terminal resistance as a function of the probe
 249 spacing between the contact points of the voltage probes on the Cu wires are
 250 shown in Figs. 8 and 9. For all of them, the probe spacing dependence of resistance
 251 basically showed a linear one-dimensional feature, meaning a diffusive
 252 transport. By multiplying the gradient of the fitted straight lines and the cross
 253 section of Cu wires (which was estimated from SEM image in Fig. 6), the three-
 254 dimensional resistivity was calculated as 4.6, 3.7, and 3.4 Ω cm, for the 70, 50 nm,
 255 and 1 μ m wide Cu wires, respectively. The resistivity of Cu increased as the line
 256 width decreased as shown in Fig. 9b. This result is understood by the Fuchs–
 257 Sondheimer theory for the surface-scattering effect and the Mayadas–Shatzkes
 258 model for the grain boundary effect [29]. No change in the measured resistance

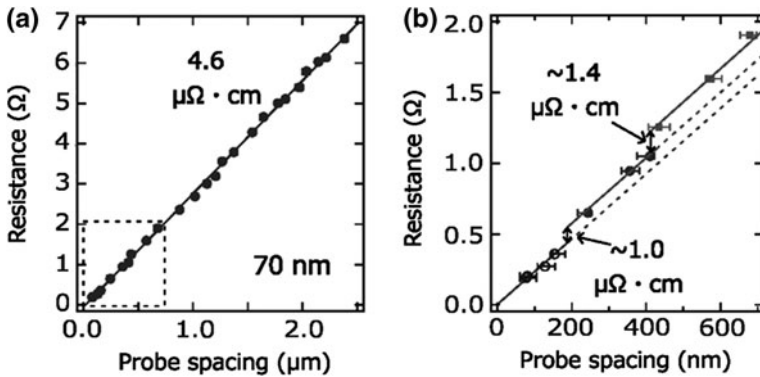


Fig. 8 **a** The measured resistances of the 70 nm wide Cu wire are shown as a function of probe spacing. **b** The enlargement of the area under 600 nm of probe spacing [29]

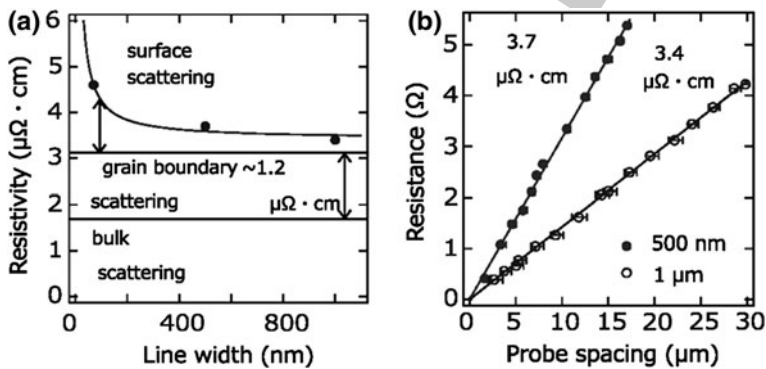


Fig. 9 **a** The measured resistances of Cu wires are shown as a function of probe spacing for the 500 nm and 1 μm wide wires. **b** Plot of the resistivity versus Cu line width [29]. The resistivity coming from the grain boundary scattering is assumed to be constant because the grain size is roughly independent of the line with in our samples

259 was found in each measurement before and after repeated contacts of CNT tips. It
 260 means no significant damage on the sample by the probe contacts.

261 In this experiment, the probe spacing was reduced to the scale which is compar-
 262 able with the grain size. Therefore, it can be expected that there will be some
 263 change in the resistance when the probe spacing becomes so short that electrons do
 264 not undergo grain boundary scattering. This has been indeed observed. Figure 8b
 265 shows the enlarged view of the data shown in Fig. 8a for the probe spacing smaller
 266 than 600 nm. There is a slight jump in resistance when the probe spacing is shorter
 267 than 200 nm. This directly corresponds to the grain boundary scattering where
 268 additional resistance occurs at the grain boundary due to the reflection of electron
 269 wave there.

6 Concluding Remarks

Electrical measurements using metal-coated CNT tips in the four-tip STM have been demonstrated for the CoSi_2 nanowires and Cu damascene wires. Since the apex of CNT tips is around 10 nm and the aspect ratio is so large, it is able to measure the resistance at nanoscale surface areas. The minimum probe spacing in the four-point probe resistance measurement was reduced to a few 10 nm, which is similar or less than the grain size of polycrystalline wires and even the carrier mean free path. The resistance along the wires present here increased linearly with the measured length, meaning classical diffusive transport. But very recently, we have found quasi-ballistic transport in semiconducting FeSi_2 nanowires at room temperature where the carrier mean free path is much longer than that of the metallic wires. The details will be reported elsewhere. In the case of Cu damascene wires, the resistivity increased as the wire width decreased. This is due to the surface/interface scattering of carrier. We have evaluated the surface/interface scattering quantitatively to obtain the specular factor in Fuchs-Sondheimer theory. At the very narrow probe spacing which was comparable to the grain size, the resistance jump due to a single grain boundary was clearly observed. As demonstrated by the measurements presented here, the four-tip STM with CNT tips is a very useful tool for transport physics at nanoscale as well as industrial purposes.

Acknowledgments The present work was done in collaboration with UNISOKU Co., Ltd. in construction of the four-tip STM and Prof. M. Katayama in fabricating CNT tips. It was fully supported by the SENTAN Program of the Japan Science and Technology Agency (JST), and also by Grants-in-Aid for Scientific Research and A3 Foresight Program from the Japanese Society for the Promotion of Science (JSPS).

References

1. Kubo, O., Shingaya, Y., Nakayama, M., Aono, M., Nakayama, T.: Epitaxially grown WO_x nanorod probes for sub-100 nm multiple-scanning-probe measurement. *Appl. Phys. Lett.* **88**, 254101 (2006)
2. Tsukamoto, S., Siu, B., Nakagiri, N.: Twin-probe scanning tunneling microscope. *Rev. Sci. Instrum.* **62**, 1767 (1991)
3. Okamoto, H., Chen, D. M.: An ultrahigh vacuum dual-tip scanning tunneling microscope operating at 4.2 K. *Rev. Sci. Instr.* **72**, 4398 (2001)
4. Watanabe, H., Manabe, C., Shigematsu, T., Shimizu, M.: Single molecule DNA device measured with triple-probe atomic force microscope. *Appl. Phys. Lett.* **78**, 2928 (2001); **79**, 2462 (2001)
5. Lin, X., He, X.B., Yang, T.Z., Guo, W., Shi, D.X., Gao, H.-J., Ma, D.D.D., Lee, S.T., Liu, F., Xie, X.C.: Intrinsic current-voltage properties of nanowires with four-probe scanning tunneling microscopy: A conductance transition of ZnO nanowire. *Appl. Phys. Lett.* **89**, 043103 (2006)
6. Guise, O., Marbach, H., Yates Jr, J.T., Jung, M.-C., Levy, J.: Development and performance of the nanoworkbench: A four tip STM for conductivity measurements down to submicrometer scales. *Rev. Sci. Instr.* **76**, 045107 (2005)
7. Ishikawa, M., Yoshimura, M., Ueda, K.: Development of four-probe microscopy for electric conductivity measurement. *Jpn. J. Appl. Phys.* **44**, 1502 (2005)

- 312 8. Takami, K., Akai-Kasaya, M., Saito, A., Aono, M., Kuwahara, Y.: Construction of independently
313 driven double-tip scanning tunneling microscope. *Jpn. J. Appl. Phys.* **44**, L120 (2005)
- 314 9. Grube, H., Harrison, B.C., Jia, J.F., Boland, J.J.: Stability, resolution, and tip-tip imaging by
315 a dual-probe scanning tunneling microscope. *Rev. Sci. Instr.* **72**, 4388 (2001)
- 316 10. Bannani, A., Bobisch, C.A., Möller, R.: Local potentiometry using a multiprobe scanning
317 tunneling microscope. *Rev. Sci. Instrum.* **79**, 083704 (2008)
- 318 11. Omicron Nano Technology GmbH (<http://www.omicron.de/>), MultiProbe, Inc (<http://www.multiprobe.com/>), Zyvex Co. (<http://www.zyvex.com/>)
- 320 12. Shiraki, I., Tanabe, F., Hobara, R., Nagao, T., Hasegawa, S.: Independently driven four-tip
321 probes for conductivity measurements in ultrahigh vacuum. *Surf. Sci.* **493**, 633 (2001)
- 322 13. Hasegawa, S., Shiraki, I., Tanabe, F., Hobara, R.: Transport at surface nanostructures
323 measured by four-tip STM. *Current Appl. Phys.* **2**, 465 (2002)
- 324 14. Hobara, R., Nagamura, N., Hasegawa, S., Matsuda, I., Yamamoto, Y., Ishikawa, K.,
325 Nagamura, T.: Variable-temperature independently-driven four-tip scanning tunneling
326 microscope. *Rev. Sci. Instr.* **78**, 053705 (2007)
- 327 15. Ikuno, T., Katayama, M., Kishida, M., Kamada, K., Murata, Y., Yasuda, T., Honda, S., Lee,
328 J.-G., Mori, H., Oura, K.: Metal-coated carbon nanotube tip for scanning tunneling
329 microscope. *Jpn. J. Appl. Phys.* **43**, L644 (2004)
- 330 16. Yoshimoto, S., Murata, Y., Hobara, R., Matsuda, I., Kishida, M., Konishi, H., Ikuno, T., Maeda,
331 D., Yasuda, T., Honda, S., Okado, H., Oura, K., Katayama, M., Hasegawa, S.: Electrical
332 characterization of metal-coated carbon-nanotube tips. *Jpn. J. Appl. Phys.* **44**, L1563 (2005)
- 333 17. Konishi, H., Murata, Y., Wongwiriyan, W., Kishida, M., Tomita, K., Motoyoshi, K.,
334 Honda, S., Katayama, M., Yoshimoto, S., Kubo, K., Hobara, R., Matsuda, I., Hasegawa, S.,
335 Yoshimura, M., Lee, J.-G., Mori, H.: High-yield synthesis of conductive carbon nanotube tips
336 for multiprobe scanning tunneling microscope. *Rev. Sci. Instr.* **78**, 013703 (2007)
- 337 18. Kanagawa, T., Hobara, R., Matsuda, I., Tanikawa, T., Natori, A., Hasegawa, S.: Anisotropy
338 in conductance of a quasi-one-dimensional metallic surface state measured by square micro-
339 four-point probe method. *Phys. Rev. Lett.* **91**, 036805 (2003)
- 340 19. Shingaya, Y., et al.: Carbon nanotube tip for scanning tunneling microscopy. *Phys. B* **323**,
341 153 (2002)
- 342 20. Ishikawa, M., et al.: Simultaneous measurement of topography and contact current by contact
343 mode atomic force microscopy with carbon nanotube probe. *Jpn. J. Appl. Phys.* **41**, 4908 (2002)
- 344 21. Ueda, K., Yoshimura, M., Nagamura, T.: A fabrication method tips for scanning probe
345 microscopes and its apparatus, Japan Patent 2004, No. 3557589
- 346 22. Tang, J., Gao, B., Geng, H., Velev, O.D., Qin, L.-C., Zhou, O.: Assembly of ID
347 nanostructures into sub-micrometer diameter fibrils with controlled and variable length by
348 dielectrophoresis. *Adv. Mater.* **15**, 1352 (2003)
- 349 23. Yoshimoto, S., Murata, Y., Hobara, R., Matsuda, I., Kishida, M., Konishi, H., Ikuno, T., Maeda,
350 D., Yasuda, T., Honda, S., Okado, H., Oura, K., Katayama, M., Hasegawa, S.: Four-point probe
351 resistance measurements using pTfR-coated carbon nanotube tips. *Nano Lett.* **7**, 956 (2007)
- 352 24. Murata, Y., Yoshimoto, S., Kishida, M., Maeda, D., Yasuda, T., Ikuno, T., Honda, S., Okado, H.,
353 Hobara, R., Matsuda, I., Hasegawa, S., Oura, K., Katayama, M.: Exploiting metal coating of
354 carbon nanotubes for scanning tunneling microscopy probes. *Jpn. J. Appl. Phys.* **44**, 5336 (2005)
- 355 25. He, Z., Smith, D.J., Bennett, P.A.: Endotaxial silicide nanowires. *Phys. Rev. Lett.* **93**, 256102 (2004)
- 356 26. Okino, H., Matsuda, I., Hobara, R., Hosomura, Y., Hasegawa, S., Bennett, P.A.: In situ resistance
357 measurements of epitaxial cobalt silicide nanowires on Si(110). *Appl. Phys. Lett.* **86**, 233108 (2005)
- 358 27. Hensel, J.C., Tung, R.T., Poate, J.M., Unterwald, F.C.: Specular boundary scattering and
359 electrical transport in single-crystal thin films of CoSi₂. *Phys. Rev. Lett.* **54**, 1840 (1985)
- 360 28. Allen, P.B., Schulz, W.W.: Bloch-Boltzmann analysis of electron transport in intermetallic
361 compounds - ReO₃, BaPbO₃, CoSi₂, and Pd₂Si. *Phys. Rev. B* **47**, 14434 (1993)
- 362 29. Kitaoka, Y., Tono, T., Yoshimoto, S., Hirahara, T., Hasegawa, S., Ohba, T.: Direct detection
363 of grain boundary scattering in damascene Cu wires by nanometer-scale four-point probe
364 resistance measurements. *Appl. Phys. Lett.* **95**, 052110 (2009)